A Projected Inverse Dynamics Approach for Multi-arm Cartesian Impedance Control

A Projected Inverse Dynamics Approach for Multi-arm Cartesian Impedance Control

Hsiu-Chin Lin, Joshua Smith, Keyhan Kouhkiloui Babarahmati, Niels Dehio, and Michael Mistry

***Abstract*— We propose a model-based control framework for multi-arm manipulation of a rigid object subject to external disturbances. The control framework, based on projected inverse dynamics, decomposes the control law into constrained and unconstrained subspaces. Unconstrained components accomplish the motion task with a desired 6-DOF Cartesian impedance behaviour against external disturbances. Meanwhile, the constrained component enforces contact and friction constraints by optimising for contact forces within the constrained subspace. External disturbances are explicitly compensated for without using force/torque sensors at the contact points. The approach is evaluated on a dual-arm platform manipulating a rigid object while coping with unknown object dynamics and human interaction.**

I. Introduction

Many activities in robotics can be described in terms of performing a desired task subject to physical *constraints* and external *disturbances*. For example, a dual-arm robot squeezing a rigid object (i.e. constraints), while a human interacts by pushing the object or adding unknown mass (i.e. disturbances) (Fig. 1). A controller must be aware of contributions from both types of forces in order to achieve its task in an optimal manner. For example, to counteract disturbances with a desired impedance response, while squeezing only as necessary to maintain contact of the object.

Several past works have considered multi-arm object manipulation [1][2], including control of the manipulated object's impedance [3][4]. A particular challenge, however, is coping with external disturbance. Maintenance of contact when grasping requires dealing with unknown forces and moments applied to the object, which may include disturbances arising from motion of the robot, unknown inertial dynamics, or the forces due to gravity. One common strategy has been to regulate the *internal* impedance of the grasp (i.e. the impedance between the end-effectors and the object) [5][6][4][7]. However, an increase in grasp force (e.g. to compensate for a forceful push) requires a displacement between the object and contact point (which does not occur with a rigid object) or an appropriate adjustment of stiffness gains and/or desired set points (which requires contact force sensing). Rather, to compute forces to maintain a grasp, we prefer to work directly in the space of contact forces, where friction cones and external forces can be explicitly, and optimally, accounted for in a constraint optimisation framework [8]. This is the approach commonly taken in locomotion [9][10], as well as in some works on grasping [11][12][13][14]).

H. Lin (Hsiu-Chin.Lin@ed.ac.uk), Joshua Smith, Keyhan Kouhkiloui Babarahmati, and Michael Mistry are at the School of Informatics, University of Edinburgh, UK. Niels Dehio is at the Research Institute for Robotics and Process Control, Technical University Braunschweig, Germany

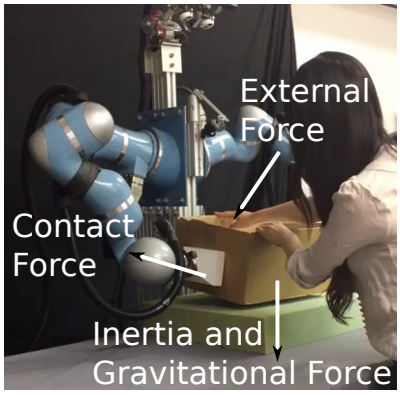

Fig. 1: A dual-arm robot manipulates an object while a human is interacting by pushing or pulling the object

In this paper, we propose a model-based controller for multi-arm manipulation of a rigid object subject to external disturbance without requiring force/torque sensors at the contact points. Our approach is as follows: we use projected inverse dynamics [15][16], such that we can design a Cartesian impedance control law in task space independently of grasp forces. Doing so allows us to estimate the contribution of external force, without knowledge of grasp forces and without the need of force/torque sensors at the contacts. Then in the orthogonal subspace, we can optimally enforce contact and friction constraints [17], without affecting the impedance characteristic, and while explicitly compensating for any disturbance forces including model error. The technique is evaluated experimentally on a dual-arm platform manipulating a rigid object of unknown mass, while receiving disturbances from a human.

The main contributions of this paper are summarised as follows:

- extending the projected inverse dynamics framework for multi-arm rigid object manipulation and grasping
- explicitly modelling external disturbances without using force/torque sensors at the contact points,
- incorporating a Cartesian impedance controller *within the unconstrained subspace* to handle external disturbances without breaking the constraints, and
- optimising contact force *within the constrained subspace* against the external disturbance without generating extra motion (which might conflict with the motion/impedance controller).

II. Background

Our work stems from prior literature in projected inverse dynamics control, impedance control, and grasping.

A. Projected Inverse Dynamics

The problem is formulated in the cartesian space projected inverse dynamics framework [16], such that the control law is decomposed into unconstrained and constrained subspaces.

Let $\mathbf{q}, \dot{\mathbf{q}}, \ddot{\mathbf{q}} \in \mathbb{R}^{\mathcal{Q}}$ denote the joint positions, velocities, and accelerations of a $\mathcal{Q}$ degree-of-freedom manipulator, the dynamics can be expressed in the Lagrangian form

$$\mathbf{M}\ddot{\mathbf{q}} + \mathbf{h} = \boldsymbol{\tau} \tag{1}$$

where $\boldsymbol{\tau} \in \mathbb{R}^{\mathcal{Q}}$ is the vector of joint torques, $\mathbf{M} \in \mathbb{R}^{\mathcal{Q}\times\mathcal{Q}}$ is the inertia matrix, and $\mathbf{h} \in \mathbb{R}^{\mathcal{Q}}$ is the vector of centrifugal, gyroscopic, and Coriolis effects, and generalised gravitational torque.

When a robot is interacting with the environment, the end-effector motion may be subject to the constraints imposed by the environment, which modifies the motion in order to accommodate the constraints. An additional term is added to describe the rigid body dynamics under constraints

$$\mathbf{M}\ddot{\mathbf{q}} + \mathbf{h} = \boldsymbol{\tau} + \mathbf{J}_c^\top \boldsymbol{\lambda}_c \tag{2}$$

where $\mathbf{J}_c \in \mathbb{R}^{\mathcal{K}\times\mathcal{Q}}$ is the constraint Jacobian that describes $\mathcal{K}$ linearly independent constraints, and $\boldsymbol{\lambda}_c$ are the constraint forces due to contact that enforce the following conditions:

$$\begin{aligned} &\mathbf{J}_c\dot{\mathbf{q}} = \mathbf{0} \\ &\mathbf{J}_c\ddot{\mathbf{q}} + \dot{\mathbf{J}}_c\dot{\mathbf{q}} = \mathbf{0}\,. \end{aligned} \tag{3}$$

[15] proposed the projected inverse dynamics framework, such that the dynamics equation in (2) may be decomposed into constrained and unconstrained components;

$$\boldsymbol{\tau} = \mathbf{P}\boldsymbol{\tau} + (\mathbf{I} - \mathbf{P})\boldsymbol{\tau} \tag{4}$$

where $\mathbf{P} = \mathbf{I} - \mathbf{J}_c^+\mathbf{J}_c$ is the orthogonal projection matrix that projects arbitrary vectors into the null space of the constraint Jacobian $\mathbf{J}_c$ and $\mathbf{J}_c^+$ is the Moore-Penrose pseudo-inverse of $\mathbf{J}_c$. Note that the two terms in (4) are orthogonal to each other $\mathbf{P}\boldsymbol{\tau} \perp (\mathbf{I} - \mathbf{P})\boldsymbol{\tau}$ such that the first term $\mathbf{P}\boldsymbol{\tau}$ generates no motion in the constraint space, and the second term $(\mathbf{I}-\mathbf{P})\boldsymbol{\tau}$ enforces the constraint without generating joint motion.

[18] introduced the *operational-space* formulation to address the dynamics of task-space movement:

$$\mathbf{F} = \boldsymbol{\Lambda}\ddot{\mathbf{x}} + \boldsymbol{\Lambda}\left(\mathbf{J}_x\mathbf{M}^{-1}\mathbf{h} - \dot{\mathbf{J}}_x\dot{\mathbf{q}}\right) \tag{5}$$

where $\mathbf{F}$ is the force applied at the end-effector for the desired acceleration $\ddot{\mathbf{x}}$, $\mathbf{J}_x$ is the Jacobian at $\mathbf{x} \in SE(3)$, and $\boldsymbol{\Lambda} = (\mathbf{J}_x\mathbf{M}^{-1}\mathbf{J}_x^\top)^{-1}$ is the operational space inertia matrix. [16] proposed operational space controllers for constrained dynamical systems such that the term $\mathbf{P}\boldsymbol{\tau}$ in (4) is replaced by $\mathbf{P}\mathbf{J}_x^\top\mathbf{F}$, and $\mathbf{F}$ is the force applied at the end-effector for the desired acceleration $\ddot{\mathbf{x}}$:

$$\mathbf{F} = \boldsymbol{\Lambda}_c\ddot{\mathbf{x}} + \boldsymbol{\Lambda}_c\left[\mathbf{J}_x\mathbf{M}_c^{-1}(\mathbf{P}\mathbf{h} - \dot{\mathbf{P}}\dot{\mathbf{q}}) - \dot{\mathbf{J}}_x\dot{\mathbf{q}}\right] \tag{6}$$

where $\boldsymbol{\Lambda}_c = (\mathbf{J}_x\mathbf{M}_c^{-1}\mathbf{P}\mathbf{J}_x^\top)^{-1}$ and $\mathbf{M}_c = \mathbf{P}\mathbf{M} + \mathbf{I} - \mathbf{P}$ are the constraint consistent operational space and joint space inertia matrix, respectively.

B. Cartesian Impedance Controller

The objective of the classical Cartesian impedance control is to dictate the disturbance response of the robot, at a particular contact location [19]. If a given operational location $\mathbf{x} \in SE(3)$ is subject to an external disturbance $\mathbf{F}_x$, we would like the resulting motion to be prescribed as

$$\mathbf{F}_x = \boldsymbol{\Lambda}_d\ddot{\tilde{\mathbf{x}}} + \mathbf{D}_d\dot{\tilde{\mathbf{x}}} + \mathbf{K}_d\tilde{\mathbf{x}} \tag{7}$$

where $\tilde{\mathbf{x}} = \mathbf{x} - \mathbf{x}_d$ and $\mathbf{x}_d$ is a virtual equilibrium point, $\boldsymbol{\Lambda}_d$, $\mathbf{D}_d$, and $\mathbf{K}_d$ are desired inertia, damping, and stiffness matrices, respectively. The control input $\mathbf{F}$ which leads to the desired impedance behaviour is given by

$$\begin{aligned} \mathbf{F} = \mathbf{h}_c + \boldsymbol{\Lambda}_c\ddot{\mathbf{x}}_d - \boldsymbol{\Lambda}_c\boldsymbol{\Lambda}_d^{-1}(\mathbf{D}_d\dot{\tilde{\mathbf{x}}} + \mathbf{K}_d\tilde{\mathbf{x}}) \\ + (\boldsymbol{\Lambda}_c\boldsymbol{\Lambda}_d^{-1} - \mathbf{I})\mathbf{F}_x \end{aligned} \tag{8}$$

where $\mathbf{h}_c$ is the operational space coriolis, centripetal, and gravity vector. If the desired inertia $\boldsymbol{\Lambda}_d$ is identical to the robot inertia $\boldsymbol{\Lambda}_c$, the feedback of the external force $\mathbf{F}_x$ can be avoided [20].

$$\mathbf{F} = \mathbf{h}_c + \boldsymbol{\Lambda}_c\ddot{\mathbf{x}}_d - \mathbf{D}_d\dot{\tilde{\mathbf{x}}} - \mathbf{K}_d\tilde{\mathbf{x}} \tag{9}$$

Using (9), the desired impedance response (7) is achieved without measuring the external force.

C. Grasping

Following the definition in [21], the grasp matrix of the i^{th} arm in a multi-arm manipulation system is defined by the mapping between the object twist to the twists of the contacts (here written with respect to a common (global) coordinate frame):

$$\mathbf{G}_i \in \mathbb{R}^{6\times6} = \begin{bmatrix} \mathbf{I}_{3\times3} & \mathbf{0}_{3\times3} \\ \mathbb{S}(\mathbf{r}_i) & \mathbf{I}_{3\times3} \end{bmatrix}$$

where $\mathbf{r}_i$ is relative distance from the contact position to the object centre-of-mass position, and $\mathbb{S}(\mathbf{r}_i) \in \mathbb{R}^{3\times3}$ is the skew-symmetric matrix performing the cross product

$$\mathbb{S}(\mathbf{r}) = \begin{bmatrix} 0 & -r_z & r_y \\ r_z & 0 & -r_x \\ -r_y & r_x & 0 \end{bmatrix}$$

Assuming that the robot has $\mathcal{K}$ manipulators, the grasp map $\mathbf{G}$ is the horizontal concatenation of $\mathcal{K}$ grasp matrices

$$\mathbf{G} \in \mathbb{R}^{6\times6\mathcal{K}} = [\mathbf{G}_1, \mathbf{G}_2, \ldots, \mathbf{G}_\mathcal{K}]$$

For example, the grasp map of the dual-arm system ($\mathcal{K} = 2$) is defined as $\mathbf{G} = \begin{bmatrix}\mathbf{G}_L & \mathbf{G}_R\end{bmatrix} \in \mathbb{R}^{6\times12}$ where $\mathbf{G}_L, \mathbf{G}_R$ are the grasp matrix of the left and the right arm.

III. Method

Our main control framework is based on extending the previous work of projected inverse dynamics control framework [16] from single arm manipulation to multi-arm manipulation, together with 6-DOF Cartesian impedance controller at the object and optimisation of constraint forces at the points of contact.

Specifically, the control law with external disturbance is decomposed into unconstrained and constrained subspaces

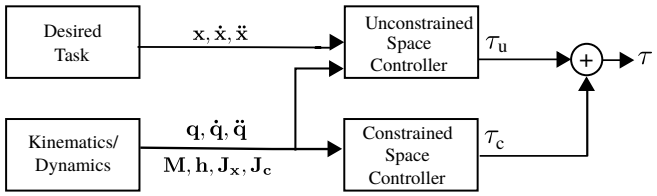

Fig. 2: An overview of the projected inverse dynamics framework

(§III-A). For multi-arm manipulation, we defined the constraints such that only internal forces are allowed in the constrained subspace (§III-B). The unconstrained subspace controller realises the underlying task and impedance behaviour (§III-C) while the constrained subspace controller estimates the contact force need to maintain the contact against external disturbance (§III-D).

A. Projected Inverse Dynamics with External disturbance

The original projected inverse dynamics does not consider external disturbance. We extended the previous work by adding an additional term for the external disturbance force $\mathbf{F}_x$ into the inverse dynamics equation (2), the general rigid-body dynamics can be described as

$$\mathbf{M}\ddot{\mathbf{q}} + \mathbf{h} = \boldsymbol{\tau} + \mathbf{J}_c^\top \boldsymbol{\lambda}_c + \mathbf{J}_x^\top \mathbf{F}_x \tag{10}$$

where $\mathbf{J}_x$ is the Jacobian that relates the joint space to the position of interaction. As only the unconstrained component of the control torque contributes to motion and the desired impedance behaviour, we multiply both sides of (10) by $\mathbf{P}$, and resulting in

$$\mathbf{P}\mathbf{M}\ddot{\mathbf{q}} + \mathbf{P}\mathbf{h} = \mathbf{P}(\boldsymbol{\tau} + \mathbf{J}_x^\top \mathbf{F}_x) \tag{11}$$

Remark The contact force $\boldsymbol{\lambda}_c$ vanished from the above equation since $\mathbf{P}\mathbf{J}_c^\top = \mathbf{0}$. An important insight is, in order to realise our desired impedance behaviour, *the unconstrained space control law does not involve the constraint force*.

Detail of $\mathbf{P}\boldsymbol{\tau}$ will be provided in §III-C. For the constraind subspace, we multiply both sides of (10) by $(\mathbf{I} - \mathbf{P})$, the dynamics can be described by

$$(\mathbf{I} - \mathbf{P})(\mathbf{M}\ddot{\mathbf{q}} + \mathbf{h}) = (\mathbf{I} - \mathbf{P})(\boldsymbol{\tau} + \mathbf{J}_x^\top \mathbf{F}_x) + \mathbf{J}_c^\top \boldsymbol{\lambda}_c \tag{12}$$

Remark The above equation aims at adding additional torque *within the constrained subspace* without any effect on the unconstrained subspace (i.e., the desired motion impedance characteristic). We can exploit this property to optmize the constraint forces required to maintain grasp of an object (see §III-D).

The notions of $\mathbf{P}$, $\mathbf{J}_c$, $\mathbf{P}\boldsymbol{\tau}$, and $(\mathbf{I} - \mathbf{P})\boldsymbol{\tau}$ are generic and can be applied to various problems of constraint systems with external disturbance. In the following sections, we will define these variables for multi-arm manipulation. For simplicity, we define $\boldsymbol{\tau}_u$ as the output from the unconstrained space controller and $\boldsymbol{\tau}_c$ as the output torque from the constraind space controller throught out this paper. An overview of the control framework is illustrated in Fig. 2.

B. Projected Inverse Dynamics for Multi-arm Manipulation

The projected inverse dynamics formulation was originally used to control single arm acting on a rigid environment. In this work, it is extended to multiple arms manipulating a single rigid object via formulating the constraints such that only *internal force* is allowed in the constrained space.

For a multi-arm robot manipulating a single rigid object via a force-closed grasp, each end-effector is in contact with the object and may generate arbitrary wrenches upon the object (see Fig. 3). The constraints are to enforce the force-closed grasp of the object and generate no motion that might violate the underlying task.

The projected inverse dynamics was built upon analytical dynamics, and based on the study in [22], the constraint force should not produce any virtual work for any virtual displacement. From the analysis in [23], *internal wrenches*, or end-effector wrench acting in the null space of grasp map (§II-C), yields the same property with constraint force in grasping. For this, the multi-arm system is constrained such that only internal wrenches are allowed to enforce the contacts.

Given a grasp map $\mathbf{G}$, the null space projection $\mathbf{I} - \mathbf{G}^+\mathbf{G}$ projects any arbitrary vector onto the null space of the grasp map. The resulting contact force satisfies $\mathbf{G}\boldsymbol{\lambda}_c = 0$, yielding no net wrench on the object and contributing to only internal force. Under this formulation, the constraint Jacobian in (16) for a multi-arm system is written as:

$$\mathbf{J}_c \in \mathbb{R}^{\mathcal{K}(\mathcal{P}\times\mathcal{Q})} = (\mathbf{I} - \mathbf{G}^+\mathbf{G}) \begin{bmatrix} \mathbf{J}_1 & & \mathbf{0} \\ & \ddots & \\ \mathbf{0} & & \mathbf{J}_\mathcal{K} \end{bmatrix} \tag{13}$$

where $\mathcal{P}$ denotes the dimensionality of the end-effector space, $\mathbf{J}_i \in \mathbb{R}^{\mathcal{P}\times\mathcal{Q}}$ are the Jacobian of the i^{th} arm, and $\boldsymbol{\lambda}_c \in \mathbb{R}^{\mathcal{K}\mathcal{P}}$ is the vertical concatenation of all contact wrenches due to internal forces that apply no net wrench on the object.

We use this constraint Jacobian $\mathbf{J}_c$ to produce the projected matrix $\mathbf{P} = \mathbf{I} - {\mathbf{J}_c}^+\mathbf{J}_c$. This projection $\mathbf{P}$ decomposes the control law such that the unconstrained component resolves the underlying task and impedance behaviour by using external forces while the constraind component maintains the contact by adding internal forces.

Remark The concept of internal/external force has been studied for multi-arm manipulating an object, (although not using the projected inverse dynamics) such as the work in [4], which uses impedance controller to control the internal force. In our work, we explicitly model the external disturbance and optimise the internal force to maintain the contact constraints against external disturbances (see §III-D).

C. Impedance Controller

In §III-A, we have shown that the dynamics in the unconstrained subspace can be described by (11). Let $\mathbf{F}_a$ be actuation force needed to accompolish the task such that $\boldsymbol{\tau} = \mathbf{J}_x\mathbf{F}_a$, the dynamics can be written as

$$\mathbf{P}\mathbf{M}\ddot{\mathbf{q}} + \mathbf{P}\mathbf{h} = \mathbf{P}\mathbf{J}_x^\top(\mathbf{F}_a + \mathbf{F}_x) \tag{14}$$

The above dynamics can also be expressed in operational space, yields (see Appendix A for details):

$$\mathbf{\Lambda}_c \ddot{\mathbf{x}} + \mathbf{h}_c = \mathbf{F}_a + \mathbf{F}_x \tag{15}$$

where $\mathbf{\Lambda}_c = (\mathbf{J}_x \mathbf{M}_c^{-1} \mathbf{P} \mathbf{J}_x^\top)^{-1}$ is the operational space inertia matrix, $\mathbf{h}_c = \mathbf{\Lambda}_c \mathbf{J}_x \mathbf{M}_c^{-1}(\mathbf{P}\mathbf{h} - \dot{\mathbf{P}}\dot{\mathbf{q}}) - \mathbf{\Lambda}_c \dot{\mathbf{J}}_x \dot{\mathbf{q}}$ is the operational space coriolis, centripetal, and gravity vector. As described in §II-B, assuming that the desired inertia is identical to the robot inertia, we can avoid the feedback of the external force $\mathbf{F}_x$, and yields

$$\boldsymbol{\tau}_u = \mathbf{P}\mathbf{J}_x^\top \mathbf{F} \tag{16}$$

where $\mathbf{F} = \mathbf{h}_c + \mathbf{\Lambda}_c \ddot{\mathbf{x}}_d - \mathbf{D}_d \dot{\tilde{\mathbf{x}}} - \mathbf{K}_d \tilde{\mathbf{x}}$ is the force needed to accompolish the underlying task and desired impedance response.

D. Optimal Contact Wrenches

In the last section, we showed that the unconstrained space controller realises the desired task and impedance behaviour without involving the constraint force. In this section, we outline our approach for the constrained space controller that attempts to apply the minimum torque required to maintain the contact without use of Force/Torque sensing at the contacts.

1) Constraints: Maintenance of the contact requires dealing with unknown forces and moments applied to the object, which may include the disturbances arising from the motion of the robot, inertial forces during manipulation, or the forces due to gravity. For this, the contact wrench applied by the hands should be sufficicient enough to prevent the separation or sliding of the contact. However, too much internal force may decrease the stability of the grasp or damage the object. Therefore, we incorporate optimisation strategies to seek the minimal contact force needed to maintain the grasp.

The contact wrench includes the contact force and the contact moment $\boldsymbol{\lambda}_c \in \mathbb{R}^6 = [\boldsymbol{\lambda}_f, \boldsymbol{\lambda}_m]^\top$. Throughout the rest of this paper, we use the subscripts f and m to denote the force and moment, respectively, and we choose the z-axis as the direction normal to the contact surface. Specifically, the contact force $\boldsymbol{\lambda}_f = [\lambda_{f,x}, \lambda_{f,y}, \lambda_{f,z}]^\top$ where $\lambda_{f,z}$ is the normal force, and $\lambda_{f,x}, \lambda_{f,y}$ are the tangential forces. The moment $\boldsymbol{\lambda}_m = [\lambda_{m,x}, \lambda_{m,y}, \lambda_{m,z}]^\top$ are the moment along each axis. A dual-arm example is illustrated in Fig. 3.

- Unilateral constraints: The manipulators should only push toward the contact, but not pull, in order to maintain contacts. Hence, the contact normal should satisfy the unilateral constraint

$$\lambda_{f,z} \geq 0 \tag{17}$$

- Friction Cone Constraints: If there is significant contact friction, a common way to describe the contact is by the Coulomb's friction model [8]. By Coulomb's Law, the magnitude of tangential force $\lambda_{f,}$ should not exceed the friction coefficient times the normal force to avoid slipping

$$\mu \lambda_{f,z} \geq \sqrt{\lambda_{f,x}^2 + \lambda_{f,y}^2} \tag{18}$$

where μ is the friction coefficient which depends on the material of the object. Geometrically, the set of forces which can be applied should lie in a cone centred about the direction normal to the contact surface (i.e. the grasp is more stable if the direction of the force is more orthogonal to the surface of the object).

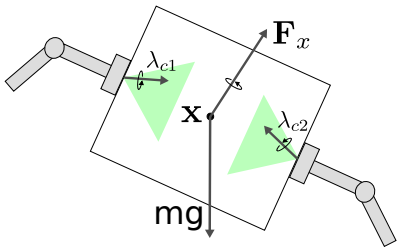

Fig. 3: An illustration of a dual-arm manipulation problem. $\mathbf{F}_x$ is an external wrench applied at operational space point $\mathbf{x}$. Other forces acting on the object include inertial and gravitational forces (e.g. mg). The contact wrenches are λ_{c1} and λ_{c2}, and their friction cones are illustrated in green. (For visualization purpose, we illustrate the contact forces and their friction cones in the opposite direction)

- Moment Constraints We assume the surface friction and the contact patch are large enough to generate friction force and moment. To avoid the hand from rolling at the contact point, the constraints are imposed on the torsional moment [12] and shear moment [13]

$$\begin{aligned} \gamma \lambda_{f,z} &\geq |\lambda_{m,z}| \\ \delta x \lambda_{f,z} &\geq |\lambda_{m,x}| \\ \delta y \lambda_{f,z} &\geq |\lambda_{m,y}| \end{aligned} \tag{19}$$

where γ is the torsional friction coefficient, and $\delta x, \delta y$ are the distance from the centre of the hand to the edge of the hand in x and y direction (assuming a rectangular contact patch). The latter two constraints ensure the contact centre of pressure remains within the contact patch of the hand.

2) Objective Function: In general, the optimisation objective is to find the minimum actuator torques needed to maintain all contacts,

$$\underset{\boldsymbol{\tau}}{\text{minimise}}\ \boldsymbol{\tau}^\top \boldsymbol{\tau}$$

Substituting $\boldsymbol{\tau}$ with $\boldsymbol{\tau}_u + \boldsymbol{\tau}_c$ from (4) and expanding the quadratic function, the objective function becomes

$$\underset{\boldsymbol{\tau}}{\text{minimise}}\ \boldsymbol{\tau}_u^\top \boldsymbol{\tau}_u + 2\boldsymbol{\tau}_u^\top \boldsymbol{\tau}_c + \boldsymbol{\tau}_c^\top \boldsymbol{\tau}_c$$

Since the unconstrained space controller $\boldsymbol{\tau}_u$ is independent of the constrained space controller $\boldsymbol{\tau}_c$ and hence is a constant during optimisation, the first term can be eliminated from the objective function.

Let $\mathbf{F}_c$ be the equivalent end-effector wrench corresponding to the input torque $\boldsymbol{\tau}_c$ such that $\boldsymbol{\tau}_c = \mathbf{J}_c^\top \mathbf{F}_c$.

Remark We can see that $\mathbf{J}_c^\top \mathbf{F}_c$ lies within the constrained manifold, i.e., $(\mathbf{I} - \mathbf{P})\mathbf{J}_c^\top \mathbf{F}_c = \mathbf{J}_c^\top \mathbf{F}_c$. It is sufficicient to enforce that the resulting torques satisfies $\boldsymbol{\tau}_c \perp \boldsymbol{\tau}_u$. The value of the second term $2\boldsymbol{\tau}_u^\top \boldsymbol{\tau}_c$ is always 0. Therefore, we can simply minimise $\boldsymbol{\tau}_c^\top \boldsymbol{\tau}_c$.

Equivalently, the objective function can be reformulated in terms of the unknown variable $\mathbf{F}_c$:

$$\underset{\mathbf{F}_c}{\text{minimise}}\ \mathbf{F}_c^\top \mathbf{J}_c\ \mathbf{J}_c^\top \mathbf{F}_c \tag{20}$$

3) Constrained optimisation: Finally, the optimisation problem is to find the optimal contact wrenches that minimises the objective function (20) while satisfying the unilateral constraints (17), the friction cone constraints (18), and the moment constraints (19) at the contact points, and balance out the external forces, including the forces acting on the object and the object dynamics.

Assuming that we have $\mathcal{K}$ contacts ($\mathcal{K} = 2$ for the dual arm example), there are $\mathcal{K}$ contact wrenches, and constraints for all the contact wrenches need to be solved. If the contact locations are fixed, finding the minimum torques is a convex optimisation problem over contact wrenches [24].

$$\begin{aligned}
&\underset{\mathbf{F}_c}{\text{minimise}}\ \mathbf{F}_c^\top \mathbf{J}_c\ \mathbf{J}_c^\top \mathbf{F}_c \\
&\text{subject to } \lambda^i_{f,z} \geq 0 \\
&\qquad \mu\lambda^i_{f,z} \geq \sqrt{(\lambda^i_{f,x})^2 + (\lambda^i_{f,y})^2} \\
&\qquad \gamma\lambda^i_{f,z} \geq |\lambda^i_{m,z}| \\
&\qquad \delta x\lambda^i_{f,z} \geq |\lambda^i_{m,x}| \\
&\qquad \delta y\lambda^i_{f,z} \geq |\lambda^i_{m,y}|
\end{aligned} \tag{21}$$

where the superscript i denotes the i^{th} contact.

Remark By setting $\boldsymbol{\tau}_c \equiv \mathbf{J}_c^\top \mathbf{F}_c$, the resulting torque satisfies $\boldsymbol{\tau}_c \perp \boldsymbol{\tau}_u$. We can simplify the objective function by removing $2\boldsymbol{\tau}_u^\top \boldsymbol{\tau}_c$ and relax the constraint $\mathbf{P}\boldsymbol{\tau}_c = \mathbf{0}$, as comparing to the optimisation problem proposed in [17].

To ensure that the acceleration generated from the constrained space controller $\boldsymbol{\tau}_c$ is consistent with the unconstrained space controller $\boldsymbol{\tau}_u$, the joint-acceleration in (12) is replaced by $\ddot{\mathbf{q}} = \mathbf{M}_c^{-1}(\boldsymbol{\tau}_u - \mathbf{P}\mathbf{h} + \dot{\mathbf{P}}\dot{\mathbf{q}})$ (See Appendix B)

$$\begin{aligned}
&(\mathbf{I} - \mathbf{P})\left[\mathbf{M}\mathbf{M}_c^{-1}(\boldsymbol{\tau}_u - \mathbf{P}\mathbf{h} + \dot{\mathbf{P}}\dot{\mathbf{q}}) + \mathbf{h} - \mathbf{J}_x^\top \mathbf{F}_x\right] \\
&= \mathbf{J}_c^\top \mathbf{F}_c + \mathbf{J}_c^\top \boldsymbol{\lambda}_c
\end{aligned} \tag{22}$$

We multiply both sides of (22) by $(\mathbf{J}_c^\top)^+$ resulting

$$\begin{aligned}
&(\mathbf{J}_c^\top)^+(\mathbf{I} - \mathbf{P})\left[\mathbf{M}\mathbf{M}_c^{-1}(\boldsymbol{\tau}_u - \mathbf{P}\mathbf{h} + \dot{\mathbf{P}}\dot{\mathbf{q}}) + \mathbf{h} - \mathbf{J}_x^\top \mathbf{F}_x)\right] \\
&\qquad = (\mathbf{J}_c^\top)^+ \mathbf{J}_c^\top \mathbf{F}_c + \boldsymbol{\lambda}_c
\end{aligned} \tag{23}$$

The left hand side can be interpreted as the sum of all external wrenches (i.e., from robot/object dynamics or human interactions) in the constrained space. Let $\boldsymbol{\eta} = (\mathbf{J}_c^\top)^+(\mathbf{I} - \mathbf{P})\left[\mathbf{M}\mathbf{M}_c^{-1}(\boldsymbol{\tau}_u - \mathbf{P}\mathbf{h} + \dot{\mathbf{P}}\dot{\mathbf{q}}) + \mathbf{h} - \mathbf{J}_x^\top \mathbf{F}_x)\right]$ and $\boldsymbol{\rho} = (\mathbf{J}_c^\top)^+ \mathbf{J}_c^\top \mathbf{F}_c$ the relationship between the contact wrench, the commanded wrench, and the external wrench can be described by a compact equality expression $\boldsymbol{\eta} = \boldsymbol{\rho} + \boldsymbol{\lambda}_c$. Each element of the contact force can be described as

$$\begin{aligned}
\lambda^i_{f,x} &= \eta^i_{f,x} - \rho^i_{f,x} \\
\lambda^i_{f,y} &= \eta^i_{f,y} - \rho^i_{f,y} \\
\lambda^i_{f,z} &= \eta^i_{f,z} - \rho^i_{f,z} \\
&\vdots
\end{aligned} \tag{24}$$

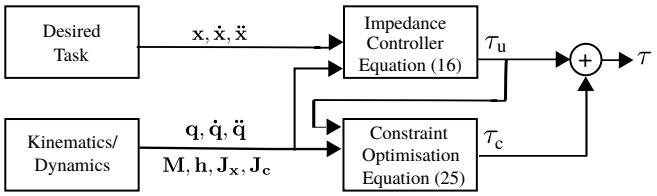

Fig. 4: An overview of the projected inverse dynamics framework

Substituting (24) into (21), the contact force $\boldsymbol{\lambda}_c$ can be eliminated from the formulation. We arrive at an optimisation problem that require minimum torques to maintain the contact forces without explicitly knowing the values of the contact forces.

$$\begin{aligned}
&\underset{\mathbf{F}_c}{\text{minimise}}\ \mathbf{F}_c^\top \mathbf{J}_c \mathbf{J}_c^\top \mathbf{F}_c \\
&\text{subject to } \eta^i_{f,z} - \rho^i_{f,z} \geq 0 \\
&\mu(\eta^i_{f,z} - \rho^i_{f,z}) \geq \sqrt{(\eta^i_{f,x} - \rho^i_{f,x})^2 + (\eta^i_{f,y} - \rho^i_{f,y})^2} \\
&\gamma(\eta^i_{f,z} - \rho^i_{f,z}) \geq |\eta^i_{m,z} - \rho^i_{m,z}| \\
&\delta x(\eta^i_{f,z} - \rho^i_{f,z}) \geq |\eta^i_{m,x} - \rho^i_{m,x}| \\
&\delta y(\eta^i_{f,z} - \rho^i_{f,z}) \geq |\eta^i_{m,y} - \rho^i_{m,y}|
\end{aligned} \tag{25}$$

Remark The optimisation problem (25) requires knowledge of the external disturbances $\mathbf{F}_x$ (included in the $\boldsymbol{\eta}$ term). Because $\mathbf{F}_x$ is estimated using the displacement of object from (7), the result of the optimisation can resist the external disturbance without using force/torque sensors.

Finally, as the friction cone constraints are quadratic (and therefore not realistic for real-time control) we approximate the constraints with linearised friction cones of 8 edges, resulting a quadratic problem with linear constraints. The constraints optimisation problem was then solved using quadratic programming [25]. During the experiment, we are able to find a solution within 1 milli-second.

Remark By decomposing the control law into two subspaces, we can impose impedance behaviour only in the unconstrained subspace without breaking the constraint (e.g., dropping the object). We can also perform constrained optimisation only within the constrained subspace, which can reduce the complexity of the optimisation problem.

In summary, we first compute $\boldsymbol{\tau}_u$, the torques needed for the desired task and impedance characteristics (16). Then, we calcualte the sum of all force acting in the constrained space $\boldsymbol{\eta}$, and then find $\boldsymbol{\tau}_c$, the minimum torque needed to maintain the contacts (25). The final output of our controller is the sum of these two $\boldsymbol{\tau} = \boldsymbol{\tau}_u + \boldsymbol{\tau}_c$. The An overview of the control framework is illustrated in Fig. 4.

IV. Evaluation

We conduct experiments using our dual KUKA LWR platform Boris. Although the robots are equipped with force/torque sensors at the end-effector, these are only used for recording forces and not in the controller.

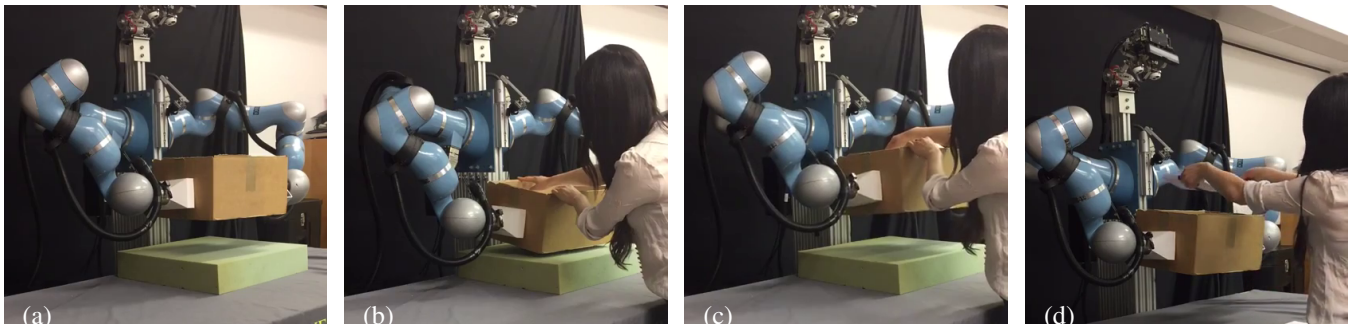

Fig. 5: Experiment of a dual-arm robot holding an object. (a) The robot holds the box in front of its torso. (b) A human pushes the box down, and (c) releases. The human adds extra weights on top of the box (d).

A. Holding an object

In this experiment, we would like to evaluate how well the robot can resist external forces. For this, the task of robot is to hold an object at a static posture while external disturbances are supplied. The robot has no knowledge about the weight of the object nor the magnitude of the external forces.

At the beginning of the experiment, as shown in Fig. 5 (a), the robot is holding a rigid box at a position in front of its torso. The size of the box is approximately $20cm \times 30cm \times 40cm$ (known to the controller) and the weight is 700 grams (unknown to the controller). A human subject pushes the box about 40 cm downward, stays for a few seconds (Fig. 5 (b)), and releases it (Fig. 5 (c)).

This process is repeated a few times, and the norm of the contact force is shown in Fig. 6 (top), where the colours denote the expected contact force (blue) and the measured contact force (red). Note that the majority of force is due to the end-effectors pushing toward each other. When the robot is at the static position, it squeezes the box with 70 N from both arms. As the person pushes the box down, the robot squeezes the box with a higher force (110 N) to prevent the box from slipping. Note that the robot does not need to measure the external forces in order to know to push harder. The external force is estimated using the displacement of the box relative to its desired position (7).

In the second half of the experiment, a human subject continuously adds extra weights on top of the box, 500 grams at a time, until a total of 2500 grams are add (see Fig. 5 (d)). The corresponding contact forces are plot in Fig. 6 (bottom). We can clearly see that the contact force increases as the total weight of the object gets heavier.

B. Manipulating an object

In our final experiment, we would like to see how well the robot reacts to external forces while performing some task. For this, the robot moves the box in a periodic trajectory, and a human attempts to interrupt the robot by holding the box at a given position (see Fig. 7).

In this experiment, the trajectory of the box is controlled. The desired trajectory is to follow the circular trajectory in y, z-plane, i.e. the desired box position is defined as $\mathbf{x}_d = [0, r\cos(st), r\sin(st)]$

Fig. 8 shows the examples of trajectory tracking in y-axis (top) and z-axis (middle). The solid lines show the true box positions and the dash lines are the desired box positions.

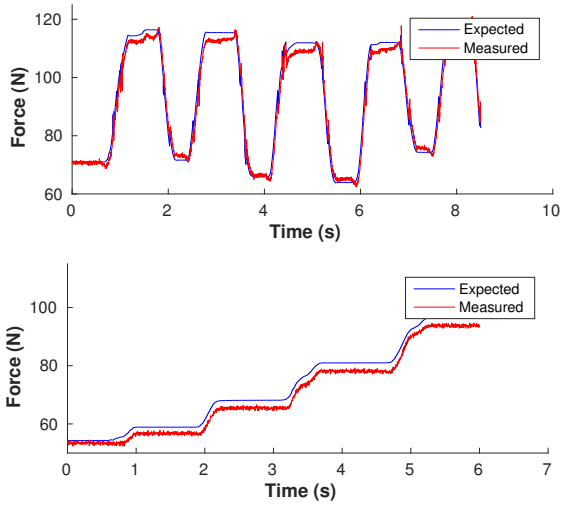

Fig. 6: Norm of the expected contact force (blue) and the measured contact force (red) for the pushing down experiment (top) and adding weights experiment (bottom). When external force increases (either by pushing or adding weight), the robot compensates by squeezing harder.

The human tries to hold the box in the middle of the plots, and therefore creates large discrepancies in both y and z axes. Once the human releases the box, the robot continues to follow the circular trajectory. Note we observe that the box positions are consistently lower than desired. Since the mass of the box is unknown to the controller, we do not compensate for its gravity and consequently the true position is always lower than desired.

The norm of the applied force is shown in Fig. 8 (bottom). We can see that the force needed to move in a circular motion varies depends on the direction of the motion, i.e. when the robot moves downward, the direction of motion is with gravity and hense less force is needed to maintain the grasp.

V. Conclusion

In this paper, a method for multi-arm manipulation with external disturbance is proposed. The problem is formulated in a projected inverse dynamics framework, such that the unconstrained (motion) controller accomplishes the task with desired impedance behaviour, and the constrained component enforces the contact in an optimal manner. The technique

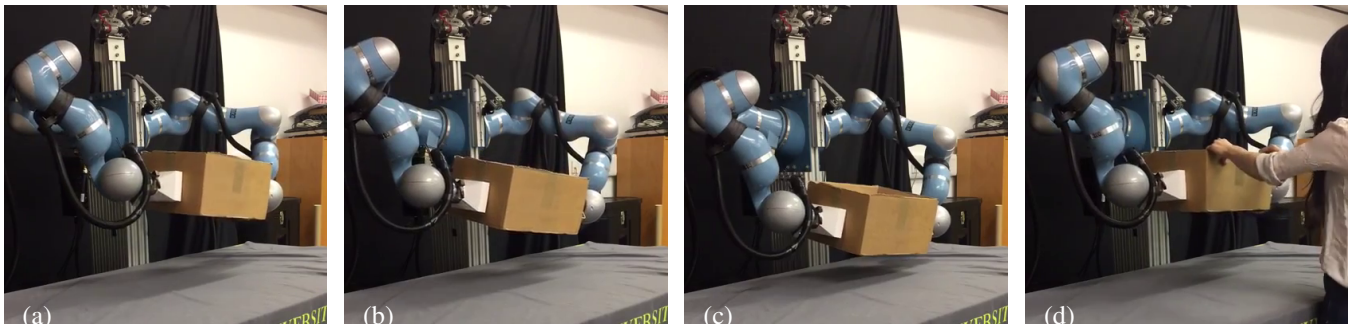

Fig. 7: Experiment of a dual-arm robot moving a box in a circular trajectory. A human attempts to break the trajectory by holding the box.

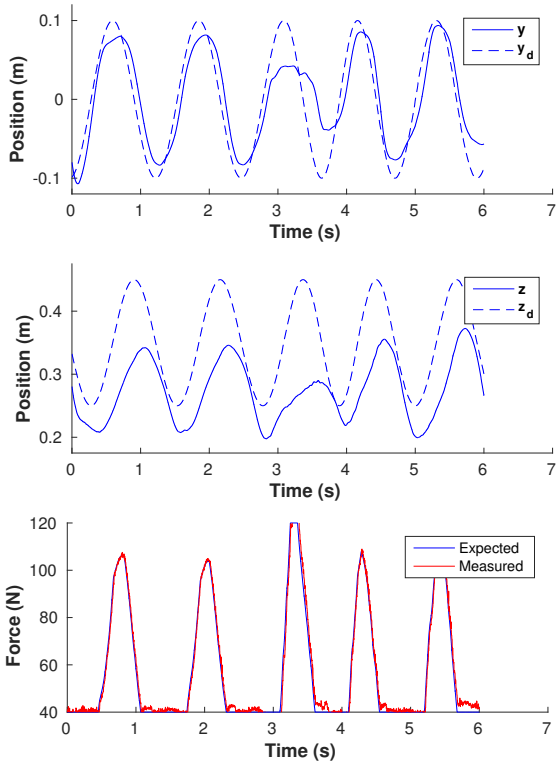

Fig. 8: A dual-arm robot moves a box in circular trajectory with human interactions. The top two figures show the trajectory tracking in y-axis and z-axis, and the bottom figure shows magnitude of expected contact force (blue) and measured contact force (red). Human interaction occurs roughly between 3 and 4 seconds.

is evaluated on a dual-arm platform, showing the proposed method's robustness to unknown disturbances. The proposed theory is generic and can be extended to multi-arms, and one of our future work is to carry out robot experiment on a multi-arm [26] and multi-leg [27] platform.

Note that throughout this work, the manipulated object is always assumed to be massless. As a consequence, any inertial or gravity forces due to mass of the object are treated as external disturbances by the impedance controller. The present work demonstrates our controller's robustness and ability to maintain a grasp, subject to unknown human interactions and unknown object inertia. However, in future work we plan to include on-line estimation of the objects mass/inertia, such that the controller may compensate for these during manipulation.

Furthermore, we have demonstrated that external disturbance forces do not need direct measurement, and may be estimated based on the displacement of the object relative to our desired impedance behaviour. This enables us to to compute optimal constraint forces without direct force measurement. In future work, however, we plan to incorporate F/T contact sensors to allow for inertia shaping in the impedance controller.

Acknowledgement

This work was funded by the European Commission Horizon 2020 Work Programme: CogIMon ICT-23-2014 644727 and THING ICT-2017-1 780883, as well as EPSRCs RAI Hubs for Extreme and Challenging Environments: ORCA EPR026173/1 and NCNR EPR02572X/1

Appendix

A. Desired end-effector Force with external disturbance

From (11), the dynamic of the unconstrained controller is described by $\mathbf{PM}\ddot{\mathbf{q}}+\mathbf{Ph}=\mathbf{P}(\boldsymbol{\tau}+\mathbf{J}_x^\top\mathbf{F}_x)$. Adding $+\dot{\mathbf{P}}\dot{\mathbf{q}}-\dot{\mathbf{P}}\dot{\mathbf{q}}$ to the left side of (11)

$$\mathbf{PM}\ddot{\mathbf{q}}+\mathbf{Ph}=\mathbf{PM}\ddot{\mathbf{q}}+\mathbf{Ph}+\dot{\mathbf{P}}\dot{\mathbf{q}}-\dot{\mathbf{P}}\dot{\mathbf{q}}$$

Using the projection matrix $\mathbf{P}$, the constraints in (3) can also be described as $(\mathbf{I}-\mathbf{P})\dot{\mathbf{q}}=\mathbf{0}$. By taking the derivative, $(\mathbf{I}-\mathbf{P})\ddot{\mathbf{q}}-\dot{\mathbf{P}}\dot{\mathbf{q}}=\mathbf{0}$. Replace the first $\dot{\mathbf{P}}\dot{\mathbf{q}}$ in the above equation by $(\mathbf{I}-\mathbf{P})\ddot{\mathbf{q}}$

$$\begin{aligned}\mathbf{PM}\ddot{\mathbf{q}}+\mathbf{Ph}&=\mathbf{PM}\ddot{\mathbf{q}}+\mathbf{Ph}+(\mathbf{I}-\mathbf{P})\ddot{\mathbf{q}}-\dot{\mathbf{P}}\dot{\mathbf{q}}\\&=(\mathbf{PM}+\mathbf{I}-\mathbf{P})\ddot{\mathbf{q}}+\mathbf{Ph}-\dot{\mathbf{P}}\dot{\mathbf{q}}\end{aligned}$$

Let $\mathbf{M}_c=\mathbf{PM}+\mathbf{I}-\mathbf{P}$, the dynamics equation in (14) can be written as

$$\mathbf{M}_c\ddot{\mathbf{q}}+\mathbf{Ph}-\dot{\mathbf{P}}\dot{\mathbf{q}}=\mathbf{P}\mathbf{J}_x^\top(\mathbf{F}_a+\mathbf{F}_x)\tag{26}$$

Multiply (26) by $\mathbf{J}_x\mathbf{M}_c^{-1}$

$$\mathbf{J}_x\ddot{\mathbf{q}}+\mathbf{J}_x\mathbf{M}_c^{-1}(\mathbf{Ph}-\dot{\mathbf{P}}\dot{\mathbf{q}})=\mathbf{J}_x\mathbf{M}_c^{-1}\mathbf{P}\mathbf{J}_x^\top(\mathbf{F}_a+\mathbf{F}_x)$$

Since $\ddot{\mathbf{x}}=\mathbf{J}_x\ddot{\mathbf{q}}+\dot{\mathbf{J}}_x\dot{\mathbf{q}}$, we replace $\mathbf{J}_x\ddot{\mathbf{q}}$ with $\ddot{\mathbf{x}}-\dot{\mathbf{J}}_x\dot{\mathbf{q}}$

$$\ddot{\mathbf{x}}-\dot{\mathbf{J}}_x\dot{\mathbf{q}}+\mathbf{J}_x\mathbf{M}_c^{-1}(\mathbf{Ph}-\dot{\mathbf{P}}\dot{\mathbf{q}})=\mathbf{J}_x\mathbf{M}_c^{-1}\mathbf{P}\mathbf{J}_x^\top(\mathbf{F}_a+\mathbf{F}_x)$$

Replacing $\boldsymbol{\tau}$ with $\mathbf{J}_x^\top \mathbf{F}_a$ where $\mathbf{F}_a$ is the actuation force needed to accompolish the task,

$$\ddot{\mathbf{x}} - \dot{\mathbf{J}}_x\dot{\mathbf{q}} + \mathbf{J}_x\mathbf{M}_c^{-1}(\mathbf{P}\mathbf{h} - \dot{\mathbf{P}}\dot{\mathbf{q}}) = \mathbf{J}_x\mathbf{M}_c^{-1}\mathbf{P}\mathbf{J}_x^\top(\mathbf{F}_a + \mathbf{F}_x)$$

Multiply by $\boldsymbol{\Lambda}_c = (\mathbf{J}_x\mathbf{M}_c^{-1}\mathbf{P}\mathbf{J}_x^\top)^{-1}$

$$\boldsymbol{\Lambda}_c\left[\ddot{\mathbf{x}} - \dot{\mathbf{J}}_x\dot{\mathbf{q}} + \mathbf{J}_x\mathbf{M}_c^{-1}(\mathbf{P}\mathbf{h} - \dot{\mathbf{P}}\dot{\mathbf{q}})\right] = \mathbf{F}_a + \mathbf{F}_x$$

Let $\mathbf{h}_c$ denotes all gravity and velocity terms such that $\mathbf{h}_c = \boldsymbol{\Lambda}_c\mathbf{J}_x\mathbf{M}_c^{-1}(\mathbf{P}\mathbf{h} - \dot{\mathbf{P}}\dot{\mathbf{q}}) - \boldsymbol{\Lambda}_c\dot{\mathbf{J}}_x\dot{\mathbf{q}}$, the operational space configuration is

$$\boldsymbol{\Lambda}_c\ddot{\mathbf{x}} + \mathbf{h}_c = \mathbf{F}_a + \mathbf{F}_x$$

If inertia shaping is avoided (see §II-B), the operational space control force is

$$\mathbf{F} = \mathbf{h}_c + \boldsymbol{\Lambda}_c\ddot{\mathbf{x}}_d - \mathbf{D}_d\dot{\tilde{\mathbf{x}}} - \mathbf{K}_d\tilde{\mathbf{x}} \tag{27}$$

B. Constraint-consistent desired acceleration

To ensure that the joint accelerations in (12) is consistent with the desired joint accelerations in (16), we need to solve $\ddot{\mathbf{q}}$ in (16). However, $\mathbf{P}$ is rank deficient, and the term $\mathbf{P}\mathbf{M}\ddot{\mathbf{q}}$ is not invertible.

From (26), the dynamics of the unconstrained space is $\mathbf{M}_c\ddot{\mathbf{q}} + \mathbf{P}\mathbf{h} - \dot{\mathbf{P}}\dot{\mathbf{q}} = \mathbf{P}\mathbf{J}_x^\top(\mathbf{F}_a + \mathbf{F}_x)$. The left-hand side is the torque needed in the unconstrained space controller. Substitute with the definition from (16),

$$\mathbf{M}_c\ddot{\mathbf{q}} + \mathbf{P}\mathbf{h} - \dot{\mathbf{P}}\dot{\mathbf{q}} = \boldsymbol{\tau}_u$$

Since $\mathbf{M}_c$ is invertible, $\ddot{\mathbf{q}}$ can be solved by

$$\ddot{\mathbf{q}} = \mathbf{M}_c^{-1}(\boldsymbol{\tau}_u - \mathbf{P}\mathbf{h} + \dot{\mathbf{P}}\dot{\mathbf{q}}) \tag{28}$$

REFERENCES

[1] S. Hayati, "Hybrid position/force control of multi-arm cooperating robots," in *IEEE International Conference on Robotics and Automation*, vol. 3. IEEE, 1986, pp. 82–89.

[2] C. Smith, Y. Karayiannidis, L. Nalpantidis, X. Gratal, P. Qi, D. V. Dimarogonas, and D. Kragic, "Dual arm manipulation - a survey," *Rob. Auton. Syst.*, vol. 60, no. 10, pp. 1340–1353, 2012.

[3] S. A. Schneider and R. H. Cannon, "Object impedance control for cooperative manipulation: Theory and experimental results," *IEEE Transactions on Robotics and Automation*, vol. 8, no. 3, pp. 383–394, 1992.

[4] F. Caccavale, P. Chiacchio, A. Marino, and L. Villani, "Six-dof impedance control of dual-arm cooperative manipulators," *IEEE/ASME Transactions On Mechatronics*, vol. 13, no. 5, pp. 576–586, 2008.

[5] R. C. Bonitz and T. C. Hsia, "Internal force-based impedance control for cooperating manipulators," *IEEE Trans. Rob. Autom.*, vol. 12, no. 1, pp. 78–89, Feb. 1996.

[6] T. Wimbock, C. Ott, and G. Hirzinger, "Impedance behaviors for two-handed manipulation: Design and experiments," in *Proceedings 2007 IEEE International Conference on Robotics and Automation*. ieeexplore.ieee.org, Apr. 2007, pp. 4182–4189.

[7] D. Heck, D. Kostić, A. Denasi, and H. Nijmeijer, "Internal and external force-based impedance control for cooperative manipulation," in *2013 European Control Conference (ECC)*. ieeexplore.ieee.org, July 2013, pp. 2299–2304.

[8] J. C. Trinkle, J.-S. Pang, S. Sudarsky, and G. Lo, "On dynamic multi-rigid-body contact problems with coulomb friction," *ZAMM-Journal of Applied Mathematics and Mechanics/Zeitschrift für Angewandte Mathematik und Mechanik*, vol. 77, no. 4, pp. 267–279, 1997.

[9] L. Righetti and S. Schaal, "Quadratic programming for inverse dynamics with optimal distribution of contact forces," in *2012 12th IEEE-RAS International Conference on Humanoid Robots (Humanoids 2012)*, Nov. 2012, pp. 538–543.

[10] Y. Lee, S. Hwang, and J. Park, "Balancing of humanoid robot using contact force/moment control by task-oriented whole body control framework," *Autonomous Robots*, vol. 40, no. 3, pp. 457–472, 2016.

[11] J. Kerr and B. Roth, "Analysis of multifingered hands," *Int. J. Rob. Res.*, vol. 4, no. 4, 1986.

[12] M. Buss, H. Hashimoto, and J. B. Moore, "Dextrous hand grasping force optimization," *IEEE Transactions on Robotics and Automation*, vol. 12, no. 3, pp. 406–418, 1996.

[13] R. G. Bonitz and T. C. Hsia, "Robust dual-arm manipulation of rigid objects via palm grasping-theory and experiments," in *IEEE International Conference on Robotics and Automation*, vol. 4. IEEE, 1996, pp. 3047–3054.

[14] A. Bicchi and V. Kumar, "Robotic grasping and contact: A review," in *IEEE International Conference on Robotics and Automation*, vol. 1. IEEE, 2000, pp. 348–353.

[15] F. Aghili, "A unified approach for inverse and direct dynamics of constrained multibody systems based on linear projection operator: applications to control and simulation," *IEEE Transactions on Robotics*, vol. 21, no. 5, pp. 834–849, 2005.

[16] M. Mistry and L. Righetti, "Operational space control of constrained and underactuated systems," *Robotics: Science and systems*, 2011.

[17] F. Aghili and C.-Y. Su, "Control of constrained robots subject to unilateral contacts and friction cone constraints," in *IEEE International Conference on Robotics and Automation*. IEEE, 2016, pp. 2347–2352.

[18] O. Khatib, "A unified approach for motion and force control of robot manipulators: The operational space formulation," *IEEE J. Robotics & Automation*, vol. 3, no. 1, pp. 43–53, 1987.

[19] N. Hogan, "Impedance control: An approach to manipulation, part i - theory," *ASME Journal of Dynamic Systems, Measurement, and Control*, vol. 107, pp. 1–7, 1985.

[20] C. Ott, *Cartesian impedance control of redundant and flexible-joint robots*. Springer, 2008.

[21] R. M. Murray, Z. Li, and S. Sastry, *A mathematical introduction to robotic manipulation*. CRC press, 1994.

[22] R. Kalaba and F. Udwadia, "Analytical dynamics with constraint forces that do work in virtual displacements," no. 2, pp. 211–217, 2001.

[23] S. Erhart and S. Hirche, "Internal force analysis and load distribution for cooperative multi-robot manipulation," *IEEE Transactions on Robotics*, vol. 31, no. 5, pp. 1238–1243, 2015.

[24] S. P. Boyd and B. Wegbreit, "Fast computation of optimal contact forces," *IEEE Transactions on Robotics*, vol. 23, no. 6, pp. 1117–1132, 2007.

[25] D. Goldfarb and A. Idnani, "A numerically stable dual method for solving strictly convex quadratic programs," *Mathematical programming*, vol. 27, no. 1, pp. 1–33, 1983.

[26] N. Dehio, J. Smith, D. L. Wigand, G. Xin, H.-C. Lin, J. J. Steil, and M. Mistry, "Modeling and control of multi-arm and multi-leg robots: Compensating for object dynamics during grasping," in *IEEE International Conference on Robotics and Automation*, 2018.

[27] G. Xin, H.-C. Lin, J. Smith, O. Cebe, and M. Mistry, "A model-based hierarchical controller for legged systems subject to external disturbances," in *IEEE International Conference on Robotics and Automation*, 2018.